



## Effects of Interface Al<sub>2</sub>O<sub>3</sub> Passivation Layer for High-*k* HfO<sub>2</sub> on GaAs

Dong Chan Suh,<sup>a,e,\*</sup> Young Dae Cho,<sup>a,\*</sup> Dae-Hong Ko,<sup>a,z</sup> Yongshik Lee,<sup>b</sup>  
Kwun Bum Chung,<sup>c</sup> and Mann-Ho Cho<sup>d</sup>

<sup>a</sup>Department of Materials Science and Engineering, <sup>b</sup>Department of Electrical and Electronics Engineering, and <sup>d</sup>Institute of Physics and Applied Physics, Yonsei University, Seoul 120-749, Korea  
<sup>c</sup>Department of Physics, Dankook University, Cheonan 330-714, Korea

The effects of Al<sub>2</sub>O<sub>3</sub> passivation, formed by atomic layer deposition (ALD) at the interface of HfO<sub>2</sub>/GaAs, were investigated by high resolution transmission electron microscopy, X-ray photoelectron spectroscopy, and capacitance–voltage (*C–V*) measurements. The results indicate that the incorporation of Ga by diffusion into the HfO<sub>2</sub> layer is reduced by the Al<sub>2</sub>O<sub>3</sub> passivation at the HfO<sub>2</sub>/GaAs interface. The Ga and As contents of the HfO<sub>2</sub> films decreased with increasing amount of interfacial Al<sub>2</sub>O<sub>3</sub> passivation, while the capacitance value decreased. The Al<sub>2</sub>O<sub>3</sub> phase optimized at five ALD cycles effectively suppressed the formation of interfacial oxide and subsequently improved the *C–V* electrical properties.

© 2010 The Electrochemical Society. [DOI: 10.1149/1.3516615] All rights reserved.

Manuscript submitted August 26, 2010; revised manuscript received October 25, 2010. Published November 19, 2010.

The development of high-*k* dielectric materials such as Al<sub>2</sub>O<sub>3</sub> (Ref. 1–4) and HfO<sub>2</sub> (Ref. 5–8) has allowed continuous complementary metal oxide semiconductor scaling by significantly reducing the extent of gate leakage current and power consumption. To realize additional high performance characteristics, semiconductors based on III–V materials with higher mobility have attracted a lot of interests to replace materials based on silicon.<sup>9,10</sup> An important issue is the direct atomic layer deposition (ALD) of HfO<sub>2</sub> on III–V materials, which continues to remain as a challenge. Passivation techniques using Si (Ref. 11 and 12) or Ge (Ref. 13 and 14) can be used to produce high quality interfaces, with equivalent oxide thickness (EOT) scalability, specifically when combined with a HfO<sub>2</sub> film. However, Si or Ge passivation on GaAs tends to result in the formation of a low-*k* interfacial oxide (SiO<sub>2</sub> or GeO<sub>2</sub>), which degrades the EOT values.

In a previous study, we reported that an Al<sub>2</sub>O<sub>3</sub> layer effectively blocked the diffusion of oxidizing species and Ga atoms into the high-*k* HfO<sub>2</sub> region, even after heat-treatment at 600°C.<sup>15</sup> Our findings indicated that, because of the presence of an interfacial Al<sub>2</sub>O<sub>3</sub> layer, not only the formation of the interfacial oxide was suppressed, but the electrical properties, including capacitance, were also improved. Despite these results, the presence of interfacial Al<sub>2</sub>O<sub>3</sub> layers poses serious problems associated with EOT scaling because the relatively low dielectric constant of Al<sub>2</sub>O<sub>3</sub> can substantially increase the EOT values of the final structures. Therefore, in order to address the issues related to scaling, it would be highly desirable to employ the process to minimize the amount of interfacial Al<sub>2</sub>O<sub>3</sub> phase between HfO<sub>2</sub> and GaAs, with still maintaining their advantages as an interfacial layer described earlier. In this study, we report on an investigation of the effects of Al<sub>2</sub>O<sub>3</sub> passivation at the HfO<sub>2</sub>/GaAs interface. Data, based on high resolution transmission electron microscopy (HR-TEM) and X-ray photoelectron spectroscopy (XPS) analysis results, as well as capacitance–voltage (*C–V*) measurement results are provided that verify the conclusions reported herein.

The substrates used in this study were 400-μm-thick p-type GaAs (100) doped with Zn [(1–4) × 10<sup>19</sup> atom/cm<sup>3</sup>]. The wafers were cleaned with a buffered oxide etcher and rinsed in deionized (DI) water. To investigate the effects of the amount of the passivating Al<sub>2</sub>O<sub>3</sub> layer, five samples were prepared with various numbers of ALD cycles for Al<sub>2</sub>O<sub>3</sub>: zero, one, three, five, and ten cycles with roughly an amount of 0.1 nm layer for each cycle. After Al<sub>2</sub>O<sub>3</sub> passivation, HfO<sub>2</sub> layer was deposited, and the total thickness of the high-*k* films was maintained at 5 nm. Both high-*k* films were formed

at a temperature of 320°C using tetrakis (ethylmethylamino) hafnium, trimethylaluminum, and DI water as reactant sources for hafnium (Hf), aluminum (Al), and oxygen (O), respectively; N<sub>2</sub> was supplied as the purge and carrier gas. After the deposition, all the samples were annealed for 1 min at 600°C by a rapid thermal process under a N<sub>2</sub> (99.9999% purity) ambient.

The microstructures of the gate dielectrics samples were examined before and after the thermal annealing process. The morphology and film thickness were examined in detail using HR-TEM and by energy-dispersive X-ray spectroscopy (EDS) analysis by scanning transmission electron microscopy with a Titan 80–300 instrument (FEI Co, Hillsboro, OR). The resolution of 0.7 nm is capable of providing very accurate atomic concentration of Ga and As in HfO<sub>2</sub>. The chemical structures of the deposited films were determined using a monochromatic XPS with an Al Kα (1486.6 eV) X-ray source. TiN gates were then formed through a standard lift-off process for the characterization of the electrical properties. Finally, *C–V* curves were acquired at 1 MHz using a B1500A LCR (Inductance, Capacitance, Resistance) meter from Agilent Technologies, Inc., Santa Clara, CA.

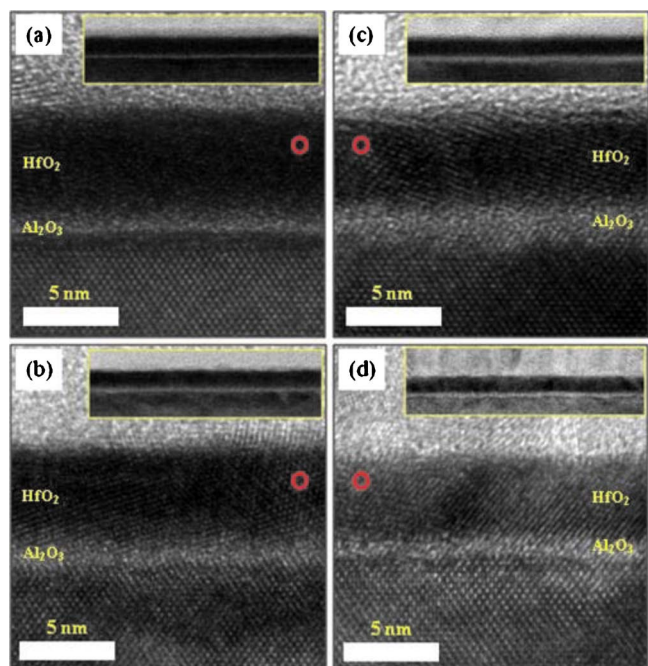
Figure 1 shows the cross sectional HR-TEM images of the HfO<sub>2</sub>/GaAs systems with ALD Al<sub>2</sub>O<sub>3</sub> passivation for one cycle and five cycles, before and after subsequent annealing. Images with a lower magnification are shown in the insets for all cases. Uniform HfO<sub>2</sub> layers with a dark contrast can be clearly seen on the GaAs in all four images. Comparison of the HR-TEM images for the two samples revealed that thermal annealing increases the thickness of the interfacial oxide layer and that this is more evident in the sample with one cycle of Al<sub>2</sub>O<sub>3</sub> deposition than in that with five cycles. Although not shown here, the transmission electron microscopy (TEM) micrograph of the samples with three cycles of Al<sub>2</sub>O<sub>3</sub> deposition showed the interfacial oxide thickness in between those with one and five cycles. Comparison of the TEM images before and after annealing indicates that due to the relatively low oxygen diffusivity of Al<sub>2</sub>O<sub>3</sub>, diffusion of impurity oxygen from the ambient gas into GaAs is blocked, suppressing the reaction between oxygen and Ga or As. Such phenomenon is more apparent as the thickness of Al<sub>2</sub>O<sub>3</sub> increases. Also, due to the interfacial oxide layers of which the formation is not completely suppressed during ALD process, the Al<sub>2</sub>O<sub>3</sub> layers in Fig. 1 is somewhat thicker than the nominal thickness of approximately 0.1 nm/cycle.

Figure 2 shows EDS spectra and the estimated Ga and As compositions for five HfO<sub>2</sub>/GaAs systems, each with different cycles of Al<sub>2</sub>O<sub>3</sub> passivation. These data clearly show that the Al<sub>2</sub>O<sub>3</sub> passivation effectively suppressed the incorporation of As and Ga into the HfO<sub>2</sub> film during the deposition and subsequent annealing. In the samples without Al<sub>2</sub>O<sub>3</sub> passivation, both Ga and As contents are measurably higher (by about 10%) after the deposition and increase

\* Electrochemical Society Student Member.

<sup>e</sup> Present address: Samsung Electronics Limited, Gyeonggi-do 445-701, Korea.

<sup>z</sup> E-mail: dhko@yonsei.ac.kr



**Figure 1.** (Color online) Cross sectional HR-TEM micrographs of  $\text{HfO}_2/\text{Al}_2\text{O}_3$ (one cycle)/GaAs systems: (a) as-deposited (b) after annealing at  $600^\circ\text{C}$  for 1 min in a  $\text{N}_2$  ambient. Cross sectional HR-TEM micrographs of  $\text{HfO}_2/\text{Al}_2\text{O}_3$ (five cycles)/GaAs systems: (c) as-deposited (d) after annealing at  $600^\circ\text{C}$  for 1 min in a  $\text{N}_2$  ambient. The circles indicate the location of sites that EDS spectra in Fig. 2 are taken. The insets are images with low magnification.

up to 15% upon annealing. The high contents are due to the incorporation of these atoms into the  $\text{HfO}_2$  films during the deposition and subsequent annealing.<sup>15</sup> In comparison, the Ga and As contents are significantly reduced to about half, even when one cycle of  $\text{Al}_2\text{O}_3$  passivation is used, and this decreases further with increased numbers of passivation cycles. In the cases of five and ten cycles, the contents of Ga and As are extremely low (not detectable for Ga and 2% for As) after deposition, and the values are maintained at the same level even after annealing, indicating that the incorporation of Ga and As into the  $\text{HfO}_2$  films is blocked almost completely, even during the annealing process.

XPS analyses were performed in order to obtain detailed information on the effects of the  $\text{Al}_2\text{O}_3$  passivating layers. Figures 3a and b show Ga 3d XPS spectra for all five samples before and after a  $\text{N}_2$

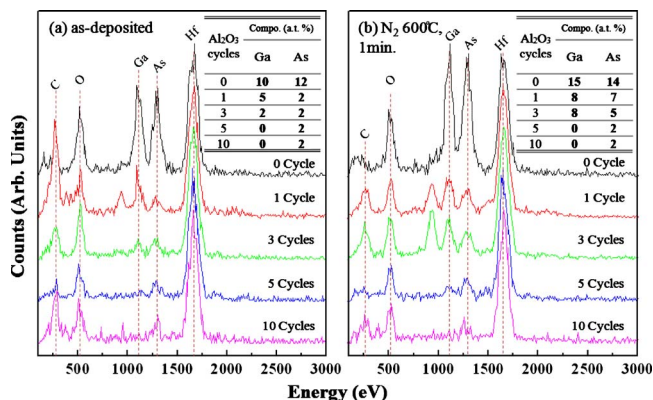
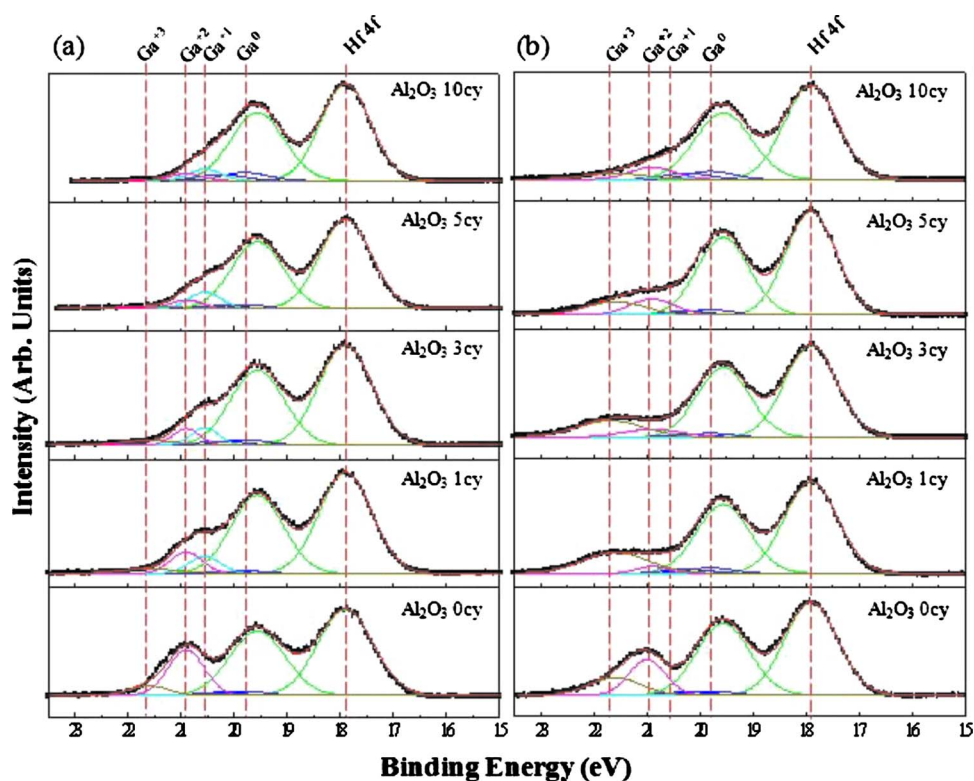


**Figure 2.** (Color online) EDS spectra of  $\text{HfO}_2/\text{Al}_2\text{O}_3/\text{GaAs}$  systems with various  $\text{Al}_2\text{O}_3$  deposition cycles: (a) as-deposited (b) after annealing at  $600^\circ\text{C}$  for 1 min in a  $\text{N}_2$  ambient.

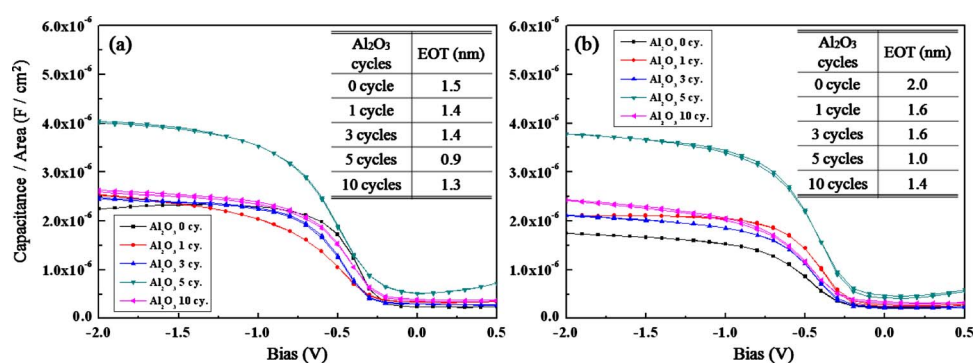
heat-treatment at  $600^\circ\text{C}$ . The peaks assigned to Hf–O and GaAs binding of the substrate ( $\text{Ga}^0$ ) are at 17.9 and 19.8 eV, respectively, whereas the peaks for Ga–O binding are at 20.5 eV for  $\text{Ga}^{+1}$  ( $\text{GaO}_x$ ), at 20.9 eV for  $\text{Ga}^{+2}$  ( $\text{Ga}_2\text{O}$ ), and at 21.7 eV for  $\text{Ga}^{+3}$  ( $\text{Ga}_2\text{O}_3$ ).<sup>17</sup> In comparison, no As–O binding was detected in the XPS analyses (data not shown). The XPS analyses results clearly demonstrate that the intensities of the peaks for Ga–O binding are significantly reduced with increasing passivation cycles in both the as-deposited and annealed samples. The amount of the Ga–O products decreased remarkably regardless of the bond states before and after annealing, even for one cycle of passivation. These results are in good agreement with the EDS analysis results for the same samples shown in Fig. 2. During the heat-treatment, GaAs reacts with oxidizing species to form Ga–O products. The oxidizing species were largely derived from diffused  $\text{HfO}_2$  and also in part from oxidizing impurities present in the  $\text{N}_2$  ambient.<sup>15,16</sup> Among the three oxidized states for Ga–O binding, the XPS spectra indicated that the amount of  $\text{Ga}^{+3}$  increased the most, regardless of the number of  $\text{Al}_2\text{O}_3$  passivation cycles employed. The  $\text{Al}_2\text{O}_3$  phase shows a higher energy of formation and a lower diffusivity of oxygen than  $\text{HfO}_2$ .<sup>18</sup> Therefore, even a small amount of  $\text{Al}_2\text{O}_3$  can behave as a passivating layer at the  $\text{HfO}_2/\text{GaAs}$  interface, as the XPS spectra indicates. As the  $\text{Al}_2\text{O}_3$  layer becomes thicker, it becomes more effective in blocking the diffusion of oxidizing species into the substrate and also Ga and As atoms into the  $\text{HfO}_2$  film. Around five cycles of  $\text{Al}_2\text{O}_3$  ALD, which corresponds to approximately 0.5 nm thickness, are sufficient to passivate effectively in a  $\text{HfO}_2/\text{GaAs}$  system, as evidenced by the EDS and XPS results.

Figure 4 shows the results of measurements of the C–V characteristic plots at 1 MHz and the calculated EOT for the samples shown in Fig. 2 and 3. In Fig. 4a, the C–V characteristics are shown for as-deposited samples with different amounts of  $\text{Al}_2\text{O}_3$  passivation. Both the samples without and with a small amount of  $\text{Al}_2\text{O}_3$  passivation (one and three cycles) showed a relatively high EOT of approximately 1.4 nm before thermal annealing, indicating that GaAs is not sufficiently passivated to suppress the incorporation of Ga and As atoms into the  $\text{HfO}_2$  films and subsequent Ga–O formation. This results in a reduction in the effective dielectric constant of  $\text{HfO}_2$ . Moreover, the post annealing process enhanced the formation of Ga–O at the interface, leading to a further increase in the EOT values. In comparison, with five deposition cycles of  $\text{Al}_2\text{O}_3$  passivation, the formation of Ga–O products is suppressed, resulting in an increase in the capacitance and therefore a relatively low EOT value of 0.9 nm. In addition, the effectiveness of the  $\text{Al}_2\text{O}_3$  passivation was also confirmed by the C–V analyses, in that the EOT value remained almost unchanged even after thermal annealing. With a further increase in the passivation cycles to ten cycles, an increase in the EOT values was observed rather than a further decrease from the case with five cycles. Such an increase can be attributed to the increase in the thickness of the  $\text{Al}_2\text{O}_3$  passivation layer, which has a smaller dielectric constant than  $\text{HfO}_2$ . These results showed that despite the effectiveness of  $\text{Al}_2\text{O}_3$  passivation as a diffusion barrier to oxidizing species as well as Ga and As atoms, the further increases of the  $\text{Al}_2\text{O}_3$  passivation over the optimum cycles (five cycles in our experiments) degrade the capacitance characteristics by increasing the EOT values of the final high- $k$  structures. It should be noted that for the more complete analyses, the characterizations of the other electrical properties such as frequency dispersions and leakage current levels should be performed in addition to our C–V data.

In summary, the effects of  $\text{Al}_2\text{O}_3$  passivation at the interface of  $\text{HfO}_2/\text{GaAs}$  were investigated.  $\text{Al}_2\text{O}_3$  passivation was found to be effective in suppressing the incorporation of Ga and As into a  $\text{HfO}_2$  film as well as the diffusion of oxidizing species before and after thermal annealing, even when a small number of passivation cycles was employed. As a result, higher capacitance values or equivalently lower EOT values were obtained as the result of  $\text{Al}_2\text{O}_3$  passivation. The optimum passivation effect was determined to be five ALD



**Figure 3.** (Color online) XPS analysis results for Ga 3d spectra of  $\text{HfO}_2/\text{Al}_2\text{O}_3/\text{GaAs}$  systems with various  $\text{Al}_2\text{O}_3$  deposition cycles (a) as-deposited and (b) at  $600^\circ\text{C}$  for 1 min in a  $\text{N}_2$  ambient.



**Figure 4.** (Color online)  $C$ - $V$  characteristics at 1 MHz before (a) and after annealing (b) for  $\text{HfO}_2/\text{Al}_2\text{O}_3/\text{GaAs}$  systems using various  $\text{Al}_2\text{O}_3$  deposition cycles.

cycles, beyond which the capacitance level decreases somewhat due to the relatively thick layer of  $\text{Al}_2\text{O}_3$  with a lower dielectric constant than  $\text{HfO}_2$ .

#### Acknowledgment

This work was financially supported by the “Next-Generation Substrate Technology for High Performance Semiconductor Devices” (no. KI002083) of the Ministry of Knowledge Economy (MKE) of Korea and “System IC 2010” project of the Korean Ministry of Science and Technology and Ministry of Commerce, Industry and Energy.

Yonsei University assisted in meeting the publication costs of this article.

#### References

- C.-W. Cheng, J. Hennessy, D. Antoniadis, and E. A. Fitzgerald, *Appl. Phys. Lett.*, **95**, 082106 (2009).
- H. D. Lee, T. Feng, L. Yu, D. Mastrogianni, A. Wan, T. Gustafsson, and E. Garfunkel, *Appl. Phys. Lett.*, **94**, 222108 (2009).
- M. Xu, Y. Q. Wu, O. Koysbasi, T. Shen, and P. D. Ye, *Appl. Phys. Lett.*, **94**, 212104 (2009).
- Y. Q. Wu, M. Xu, P. D. Ye, Z. Cheng, J. Li, J.-S. Park, J. Hydrick, J. Bai, M. Carroll, J. G. Fiorenza, and A. Lochtefeld, *Appl. Phys. Lett.*, **93**, 242106 (2008).
- C. Y. Kim, S. W. Cho, M.-H. Cho, K. B. Chung, D. C. Suh, D.-H. Ko, C.-H. An, H. Kim, and H. J. Lee, *Appl. Phys. Lett.*, **95**, 042903 (2009).
- É. O’Connor, S. Monaghan, R. D. Long, A. O’Mahony, I. M. Povey, K. Cherkaoui, M. E. Pemble, G. Brammertz, M. Heyns, S. B. Newcomb, et al., *Appl. Phys. Lett.*, **94**, 102902 (2009).
- G. K. Dalapati, A. Sridhara, A. S. W. Wong, C. K. Chia, and D. Z. Chi, *Appl. Phys. Lett.*, **94**, 073502 (2009).
- R. Suri, D. J. Lichtenwalner, and V. Misra, *Appl. Phys. Lett.*, **92**, 243506 (2008).
- International technology roadmap for semiconductors (2009), <http://www.itrs.net>, last accessed August 15, 2010.
- R. W. Keys, *Science*, **195**, 1230 (1997).
- S. Suthram, Y. Sun, P. Majhi, I. Ok, H. Kim, H. R. Harris, N. Goel, S. Parthasarathy, T. Koehler, T. Acosta, et al., *Dig. Tech. Pap.—Symp. VLSI Technol.*, **2008**, 182.
- I. Ok, H. Kim, M. Zhang, F. Zhu, S. Park, J. Yum, H. Zhao, D. Garcia, P. Majhi, and J. C. Lee, *Appl. Phys. Lett.*, **92**, 202908 (2008).
- G. K. Dalapati, A. Sridhara, A. S. W. Wong, C. K. China, S. J. Lee, and D. Chi, *Appl. Phys. Lett.*, **91**, 242101 (2009).
- H.-S. Kim, I. Ok, M. Zhang, F. Zhu, S. Park, J. Yum, H. Zhao, J. C. Lee, P. Majhi, N. Goel, et al., *Appl. Phys. Lett.*, **93**, 062111 (2008).
- D. C. Suh, Y. D. Cho, S. W. Kim, D.-H. Ko, Y. Lee, M.-H. Cho, and J. Oh, *Appl. Phys. Lett.*, **96**, 142112 (2010).
- D. C. Suh, Y. D. Cho, Y. Lee, D.-H. Ko, K. B. Chung, and M.-H. Cho, *Electrochem. Solid-State Lett.*, **12**, H376 (2009).
- H.-S. Kim, I. Ok, M. Zhang, F. Zhu, S. Park, J. Yum, H. Zhao, J. C. Lee, J. Oh, and P. Majhi, *Appl. Phys. Lett.*, **92**, 102904 (2008).
- C. Y. Kim, S. W. Cho, M.-H. Cho, K. B. Chung, C.-H. An, H. Kim, H. J. Lee, and D.-H. Ko, *Appl. Phys. Lett.*, **93**, 192902 (2008).